



Published in final edited form as:

JACC Heart Fail. 2014 February 1; 2(1): 49–61. doi:10.1016/j.jchf.2013.08.008.

Human Cardiosphere-Derived Cells From Advanced Heart Failure Patients Exhibit Augmented Functional Potency in Myocardial Repair

Ke Cheng, PhD^{#*}, Konstantinos Malliaras, MD^{#*}, Rachel Ruckdeschel Smith, PhD^{#*,†}, Deliang Shen, MD, PhD^{*,‡}, Baiming Sun, MS^{*}, Agnieszka Blusztajn, BS[†], Yucai Xie, MD, PhD^{*}, Ahmed Ibrahim, MS^{*}, Mohammad Amin Aminzadeh, MD^{*}, Weixin Liu, MS^{*}, Tao-Sheng Li, MD, PhD^{*,§}, Michele A. De Robertis, BS^{*}, Linda Marbán, PhD^{*,†}, Lawrence S. C. Czer, MD^{*}, Alfredo Trento, MD^{*}, and Eduardo Marbán, MD, PHD^{*}

^{*}Cedars-Sinai Heart Institute, Los Angeles, California

[†]Capricor Inc., Los Angeles, California

[‡]Department of Cardiology, The First Affiliated Hospital of Zhengzhou University, Zhengzhou, People's Republic of China

[§]Department of Stem Cell Biology, Nagasaki University Graduate School of Biomedical Science, Nagasaki, Japan.

[#] These authors contributed equally to this work.

Abstract

Objectives—This study sought to compare the regenerative potency of cells derived from healthy and diseased human hearts.

Background—Results from pre-clinical studies and the CADUCEUS (Cardiosphere-Derived Autologous stem Cells to reverse ventricular dysfunction) trial support the notion that cardiosphere-derived cells (CDCs) from normal and recently infarcted hearts are capable of regenerating healthy heart tissue after myocardial infarction (MI). It is unknown whether CDCs derived from advanced heart failure (HF) patients retain the same regenerative potency.

Methods—In a mouse model of acute MI, we compared the regenerative potential and functional benefits of CDCs derived from 3 groups: 1) non-failing (NF) donor: healthy donor hearts post-transplantation; 2) MI: patients who had an MI 9 to 35 days before biopsy; and 3) HF: advanced cardiomyopathy tissue explanted at cardiac transplantation.

Results—Cell growth and phenotype were identical in all 3 groups. Injection of HF CDCs led to the greatest therapeutic benefit in mice, with the highest left ventricular ejection fraction, thickest infarct wall, most viable tissue, and least scar 3 weeks after treatment. In vitro assays revealed that HF CDCs secreted higher levels of stromal cell-derived factor 1 (SDF-1), which may contribute to the cells' augmented resistance to oxidative stress, enhanced angiogenesis, and improved myocyte survival. Histological analysis indicated that HF CDCs engrafted better, recruited more

© 2014 by the American College of Cardiology Foundation Published by Elsevier Inc.

Reprint requests and correspondence: Dr. Eduardo Marbán, Cedars-Sinai Heart Institute, 8700 Beverly Boulevard, Los Angeles, California 90048. Marban@csmc.edu OR Dr. Ke Cheng, Department of Molecular Biomedical Science, North Carolina State University, 1060 William Moore Drive, Raleigh, North Carolina 27607. ke_cheng@ncsu.edu..

Current affiliation for Dr. Cheng: Department of Molecular Biomedical Science at North Carolina State University and UNC/NCSU Joint Department of Biomedical Engineering, Raleigh, North Carolina.

All other authors have reported that they have no relationships relevant to the contents of this paper to disclose.

endogenous stem cells, and induced greater angiogenesis and cardiomyocyte cell-cycle re-entry. CDC-secreted SDF-1 levels correlated with decreases in scar mass over time in CADUCEUS patients treated with autologous CDCs.

Conclusions—CDCs from advanced HF patients exhibit augmented potency in ameliorating ventricular dysfunction post-MI, possibly through SDF-1-mediated mechanisms.

Keywords

cardiosphere-derived cells; heart failure; myocardial infarction; patient characteristics; stromal cell-derived factor 1

Extensive pre-clinical studies of cardiosphere-derived cells (CDCs) have recently culminated in the first-in-human CADUCEUS (CARDiosphere-Derived aUtologous stem CELls to reverse ventricUlar dySfunction) trial (1). CDCs are intrinsic to the heart (2), express a distinctive profile of antigens (>98% CD105⁺, <0.5% CD45⁺) (3,4), and promote cardiac regeneration after ischemic injury. In animal models of myocardial infarction (MI), CDCs temporarily engraft (5–8) and exert strong bystander effects leading to the recruitment of endogenous stem cells (5,6,9), attenuation of apoptosis in the host myocardium (3,6,9,10), stimulation of cardiomyocyte cell-cycle re-entry (3,6,11,12), promotion of angiogenesis (5,6), and production of long-lasting functional benefits (2,4–6,9,10,13–18).

So far, CDCs have been derived from nominally healthy (post-transplantation donor hearts) or moderately dysfunctional (post-MI) hearts. It is unknown whether CDCs from end-stage heart failure (HF) patients retain comparable therapeutic potential. Also, no previous study has performed direct head-to-head comparison of CDCs (or any other heart-derived cells) from patients with varying severities of cardiac dysfunction. Here, we compared the in vitro properties and in vivo regenerative potential of CDCs derived from non-failing (NF) donor, acute MI, and failing heart tissues. We further evaluated potential roles for various secreted growth factors in product potency, and correlated the levels of each of these factors with structural remodeling in CDC-treated CADUCEUS patients.

Methods

A detailed description of the methods can be found in the Online Appendix.

Donor comorbidity and study design

Patient characteristics from the 3 groups are shown in Table 1. NF donor CDCs were derived from endomyocardial biopsies of donor hearts after transplantation. The hearts had been exposed to various regimens of immunosuppressive drugs but were otherwise healthy and free of cardiomyopathy. MI CDCs were derived from endomyocardial biopsies of acute MI patients enrolled in the CADUCEUS trial (harvested 9 to 35 days post-MI). Most of these patients were New York Heart Association (NYHA) functional class I, and the remaining were class II. HF CDCs were derived from myocardial samples of failing hearts from heart transplant or ventricular assist device recipients. All HF patients were NYHA functional class IV, with various types of cardiomyopathy.

CDCs were derived as described (3,4) (n = 6 donors for each group). Passage 2 cells were used for all studies. Expression of surface markers was assessed by flow cytometry. Enzyme-linked immunosorbent assay (ELISA) and reverse transcription–polymerase chain reaction (RT-PCR) were performed to measure secreted factors and expression of key genes, respectively. The terminal deoxynucleotidyl transferase dUTP nick end labeling (TUNEL) assay was performed to measure cell apoptosis under oxidative stress. Endothelial cell tube

formation assay was conducted to evaluate angiogenesis. A total of 100,000 cells were intramyocardially injected into the border zone of SCID mice immediately after myocardial infarction (left anterior descending coronary artery ligation). Echocardiography was performed at baseline and 3 weeks afterwards to measure left ventricular ejection fraction (LVEF). Afterwards, animals were euthanized and histology was performed to evaluate cell engraftment, differentiation, and stimulation of endogenous repair. Comparison between groups was conducted by 1-way analysis of variance followed by post hoc Bonferroni test.

Results

CDC morphology, growth, and phenotype from the 3 donor groups

With a 3-stage processing protocol (explants, cardiospheres, and replating) (4), CDCs could be readily derived and expanded from all groups including HF tissues. Cell morphologies at all stages were identical for all groups (Fig. 1A). As a measure of cell growth and proliferation, population doublings over time and averaged doubling times were calculated (Fig. 1B). No differences were found among the 3 groups, indicating that the generation and expansion of CDCs was not affected by the diseases in question.

Flow cytometry was performed to characterize the antigenic profile of CDCs from the different patient groups. As per the product release criteria for the CADUCEUS trial (1), CDCs are consistently positive for CD105 (a TGF- β receptor subunit) and negative for CD45 (a pan-hematopoietic marker) (Fig. 1D). A small fraction (<10%) of CDCs expresses the stem cell marker c-kit (CD117) in all groups (Fig. 1D). Another very small fraction of CDCs expresses DDR2, a cardiac fibroblast marker (Fig. 1D), in all groups. In sum, the antigenic profiles of CDCs from different patient groups are comparable.

Therapeutic benefits in mice with myocardial infarction

2,3,5-triphenyltetrazolium chloride (TTC) staining revealed superior myocardial tissue viability in hearts that had been injected with HF CDCs (Fig. 2A, red bar in the graph). Trends suggest that NF donor CDC or MI CDC therapies may also reduce acute injury as compared with Control injections, but the differences are not statistically significant. TUNEL staining revealed decreases of apoptosis (TUNEL⁺ nuclei) in all 3 cell-injected groups, with the greatest protection seen in the HF CDC group (Fig. 2B). These data manifest a cardioprotective effect of CDCs in acute MI that is augmented in HF CDCs.

Heart morphometry at 3 weeks showed severe left ventricular (LV) chamber dilation and infarct wall thinning in the Control hearts (Fig. 3A, upper panel). By contrast, all the CDC-treated groups exhibited some degree of attenuated LV remodeling (Fig. 3A, upper panels). Snapshots of the infarct border zone showed extensive scar (blue) and only partial preservation of viable myocardium (red) in Control hearts. By contrast, the CDC-treated hearts exhibited readily evident therapeutic benefit (i.e., more viable myocardium and less scar tissue) (Fig. 3A, lower panels). Compared with Control (Figs. 3B to 3E, white bars), injection of NF donor CDCs (Figs. 3B to 3E, gray bars) or MI CDCs (Figs. 3B to 3E, blue bars) increased the minimal infarct wall thickness (Fig. 3B) and viable tissue mass (Fig. 3D) while decreasing scar mass (Fig. 3C) and scar size (Fig. 3E) 3 weeks after treatment. The salutary effects were even greater in HF CDC-treated hearts, which had the thickest infarcted walls, smallest scars, and largest amount of viable tissue among all groups (Figs. 3B to 3E, red bars).

A consistent indicator of cell potency in this model is the ability to produce functional benefit after transplantation (3,4,6,11). LVEF values at baseline (i.e., 4 h post-infarction) were comparable, indicating similar degrees of ischemic injury among groups (Fig. 3F). Over the 3-week time course of observation, LVEF deteriorated in the Control group (Fig.

3G, white bar), but NF donor CDC (consistent with previous studies [3,4,6,11]) or MI CDC injection preserved LVEF. HF CDCs actually resulted in a sizable boost in LVEF ($p < 0.05$ vs. all other groups) (Fig. 3G). Representative echocardiographic images are shown in Figure 3H. Taken together, these data show that CDCs derived from HF patients were not compromised in their therapeutic potential. Indeed, advanced cardiomyopathy confers augmented regenerative potency.

Paracrine factor secretion, cardiac and extracellular matrix gene expression, and proteolytic activity

Paracrine mechanisms underlie many of the beneficial effects of CDC transplantation (6,9,10). Consistent with our previous findings (17), CDCs secreted various growth factors (Figs. 4A to 4D), but HF CDCs produced higher amounts of stromal cell-derived factor 1 (SDF-1) (Fig. 4D) than did NF donor or MI CDCs. To see whether HF CDCs produce more inflammatory cytokines, we measured monocyte chemoattractant protein-3 (MCP-3), leptin, and interleukin 6 (IL-6) in the conditioned media (CM). There was no statistical difference among the 3 CDC groups (Figs. 4F to 4H). No statistical differences in metalloproteinase activities (MMP2/MMP9) were found among the 3 CDC groups (Fig. 4I). RT-PCR revealed that the expression levels of cardiac (*GATA4*, *MEF2C*) and extracellular matrix genes (laminin beta 1 [*LAMBI*]) were indistinguishable in all 3 CDC groups (Figs. 4J to 4L). Also, HF CDC injection led to a robust increase of myocardial SDF-1 tissue level (Fig. 4M), confirming and extending the in vitro analyses. In sum, we found that HF CDCs produced more SDF-1 than did CDCs from the other 3 groups; all other measures were similar.

Resistance to oxidative stress

Enhanced cell resistance to oxidative stress favors transplanted cell engraftment and greater functional benefit (10). After 24 h of exposure to 100 $\mu\text{mol/l}$ H_2O_2 , the number of apoptotic cells was lower in HF CDCs than in NF donor or MI CDCs (Figs. 5A and 5B). To test the role of SDF-1 in this enhanced protection against oxidative stress, SDF-1 inhibitor AMD3100 was added into HF CDC culture. The percentage of apoptotic cells increased, indicating impaired resistance to oxidative stress. Conversely, adding recombinant human SDF-1 to NF donor CDCs decreased the percentage of apoptotic cells. These results suggest that HF CDCs are more resistant to oxidative stress than are NF donor or MI CDCs, at least partially through SDF-1-mediated cell protection.

Angiogenesis assay

We evaluated the pro-angiogenic potency of CDCs using an in vitro endothelial cell tube-forming assay. Human umbilical vein endothelial cells (HUVECs) cultured in vascular cell growth medium formed nice tubes on Matrigel BD Biosciences, Franklin Lakes, NJ within 6 h, whereas tube formation was diminished in basal medium (BM) not containing pro-angiogenic growth factors (Fig. 5C). CM from all 3 CDC groups enhanced tube formation as compared with BM (Fig. 5C). Quantitative analysis showed that cumulative tube length was greater in HF CDC CM than in NF donor or MI CDC CM (Fig. 4D). Adding recombinant human SDF-1 into BM enhanced tube formation, consistent with the idea that SDF-1 may contribute to the enhanced pro-angiogenic effects of HF CDC CM.

Cardiomyocyte survival assay

We examined the effects of CDC CM on the survival and contractility of ex vivo-cultured cardiomyocytes. Neonatal rat cardiomyocytes (NRCMs) were cultured in plain Iscove's modified Dulbecco's medium (IMDM) (negative control) or IMDM conditioned by CDCs. After 3 days in culture, NRCMs in plain IMDM rounded up and started to detach from the surface (Fig. 5E, Plain Media panel). By contrast, NRCMs in CDC CM (Fig. 5E, top 3

panels) showed a higher survival rate and were widely spread out with clear striations (Fig. 5E, Snapshot panel). Quantitative analysis indicated a greater number of NRCMs in HF CDC CM after 3 days in culture than in NF donor or MI CDC CM (Fig. 5F).

To explore the role of SDF-1 in cardiomyocyte survival, SDF-1 inhibitor AMD3100 was added to the culture. Interestingly, the CDC-mediated cardiomyocyte survival privilege was largely abolished (Figs. 5E, middle 3 panels, and 5F), with only a few surviving NRCMs after 3 days of culture. Conversely, adding recombinant rat SDF-1 into IMDM rescued most of the cells (Figs. 5E, IMDM + SDF-1 panel, and 5F). However, the NRCM size was smaller than in CDC CM, suggesting that factors other than SDF-1 are also important in maintaining normal cardiomyocyte morphology.

Engraftment and differentiation of injected CDCs

CDC engraftment in mouse hearts 3 weeks after injection was evaluated using human-specific nuclear antigen (HNA) as the marker. Consistent with our previous findings, a few HNA⁺ cells could be detected in all groups (Fig. 6A, green cells indicated by white arrows). Although the absolute number was small, engraftment (i.e., the number of HNA⁺ cells) was greater in mouse hearts implanted with HF CDCs than in those injected with NF donor or MI CDCs. Histology revealed expression of alpha-sarcomeric actin (α -SA), smooth muscle actin (SMA), and von Willebrand factor (vWF) in some of the surviving progeny of human CDCs (HNA⁺ cells), confirming the ability of HF CDCs to differentiate into all 3 major cardiovascular lineages in vivo (Figs. 6B and 6C). To assess exogenous and endogenous myocyte formation, we counted cardiomyocytes of either human (α -SA⁺/HNA⁺) or mouse origin (α -SA⁺/HNA⁻) in the peri-infarct area. HF CDC therapy resulted in an overall boost of myocyte number as compared with Control, NF donor, or MI CDC therapies (Fig. 6E). Interestingly, the vast majority of myocytes were of endogenous origin (red bars). With the current model, it is impossible to determine whether the increase in myocyte number is due to cardioprotection or to regeneration. Nevertheless, more human-derived myocytes (green bars) were found in the hearts that received HF CDCs than in the other 2 cell therapy groups, consistent with the superior cell engraftment seen in the HF CDC group.

Indirect repair: stem cell recruitment, cardiomyocyte proliferation, and angiogenesis

Although HF CDCs engrafted more than did NF donor or MI CDCs, these “needle in the haystack” instances of direct differentiation events cannot account for the observed robust functional benefit. We thus attempted to evaluate indirect repair mechanisms triggered by the transplantation of CDCs. Possible mechanisms include recruitment of endogenous progenitor cells to the site of cell transplantation (19,20), cardiomyocyte cell-cycle re-entry (6), and angiogenesis (21). c-kit⁺ (green) and CD34⁺ (magenta) cells could be detected in the infarct border zone (Fig. 7A). Greater numbers of c-kit⁺ and CD34⁺ cells were found in the hearts that had received HF CDCs than in NF donor or MI CDC groups (Fig. 7B). Higher magnification revealed interactions (yellow arrow) between transplanted HF CDCs and c-kit⁺ (Fig. 7C) or CD34⁺ cells (Fig. 7D). Some c-kit⁺ (Fig. 7E, white arrow) and CD34⁺ (Fig. 7F, white arrow) cells co-expressed CXCR4, the receptor of SDF-1, rendering plausible the notion that they might be recruited via the SDF-1/CXCR4 axis. An additional role for proliferation of existing cardiomyocytes (22,23) is supported by the finding of more ki67⁺ cardiomyocytes (Figs. 7G, white arrows, and 7H) in hearts transplanted with HF CDCs. Moreover, HF CDC transplantation boosted angiogenesis. Arteriolar density, identified by immunostaining for SMA, was markedly increased 3 weeks after HF CDC therapy compared with NF donor or MI CDCs (Figs. 7I and 7J). Moreover, HF CDC-injected hearts exhibited the greatest number of cycling endothelial cells (ki67⁺/vWF⁺), which were detected in small, medium, and large vessels (Figs. 7K and 7L).

Correlation of CDC properties with therapeutic outcomes in patients

In the CADUCEUS trial, sizable decreases in scar mass and increases in viable cardiac mass (measured by contrast-enhanced magnetic resonance imaging) were observed at 6 and 12 months post-CDC therapy, but not in control subjects (1). We performed linear regression analysis in the 6 MI CDC patients, correlating the measured levels of each growth factor in CDC CM and gene expression levels with changes in scar mass or viable mass at 6 months in the same patient. SDF-1 levels correlated negatively with the time-dependent changes in scar mass (Fig. 8A) ($R^2 = 0.68$, $p = 0.04$). No other significant correlation was detected between growth factor levels and changes in scar mass at 6 months (Figs. 8B to 8I).

Discussion

CDCs represent an attractive cell type for cardiac repair. Over the past 9 years, we and others have demonstrated CDCs' capability to augment cardiac function and myocardial viability in mouse, rat, and pig models of MI (3–7,9–11,13,15–17). Moreover, a proof-of-concept study using autologous CDCs, the CADUCEUS trial, has yielded the first clinical evidence for therapeutic regeneration (1). We have also demonstrated the comparable safety and efficacy of allogeneic cell therapy in infarcted rats transplanted with mismatched CDCs without immunosuppression (6). The tissue sources for allogeneic CDC therapy can be expanded if functionally competent CDCs can be derived from hearts with existing cardiomyopathy. A recent report highlighted that c-kit⁺ cardiac stem cells can be isolated from endomyocardial biopsies of patients with advanced cardiomyopathy (24).

Toward these ends, we derived CDCs from hearts with advanced cardiomyopathy (HF CDCs) and compared their in vitro characteristics and regenerative potency with CDCs from healthy (NF donor CDCs) or post-MI donor hearts (MI CDCs). We first demonstrated that CDCs could be readily derived from all 3 patient groups. The growth rates and phenotypes of HF CDCs were similar to those of NF donor and MI CDCs (Fig. 1).

We then tested the regenerative potency of NF donor, MI, and HF CDCs in a mouse model of acute MI. Until now, the prevailing wisdom has been that young and healthy donor hearts are preferable as the tissue source for cell therapy (25). Surprisingly, we found that HF CDCs outperformed NF donor and MI CDCs in acute cardiac protection (Fig. 2), and in attenuating LV remodeling and boosting cardiac function (Fig. 3). Thus, the therapeutic potential of CDCs was not compromised by advanced cardiomyopathy; indeed, end-stage HF seemed to confer superior functional potency on CDCs. We considered the possibility that advanced cardiomyopathy may boost the number of stem cells in the limited viable tissue (26,27) and thereby confer higher potency on CDCs. However, flow cytometry analysis (Fig. 1) indicated that putative stem cell subpopulations were similar in all 3 groups. We then switched our focus to paracrine mechanisms. ELISA revealed that HF CDCs produced higher levels of SDF-1 (Fig. 4D) as compared with NF donor or MI CDCs. The mechanisms underlying elevated SDF-1 production in HF CDCs are unclear. Elevated serum levels of SDF-1 protein, and RNA levels of myocardial SDF-1, have been reported in ischemic HF patients (28,29). SDF-1 is believed to be beneficial in ischemic cardiomyopathy (30–35) by promoting various mechanisms: 1) angiogenesis (33,36–38); 2) cell survival (for both stem cells and cardiomyocytes) (39–42); 3) proliferation (43); 4) migration (i.e., recruitment of stem cells) (44,45). We therefore performed a series of in vitro and in vivo studies to test whether these mechanisms might underlie the superior potency of HF CDCs. In vitro, we found that HF CDCs were more resistant to oxidative stress (Figs. 5A and 5B). HF CDC CM was superior in promoting tube formation by endothelial cells (Figs. 5C and 5D) and the survival of cardiomyocytes (Figs. 5E and 5F). Introducing recombinant SDF-1 into nonconditioned culture medium at least partially mimicked the superior effects of HF-CDCs. Conversely, inhibiting SDF-1 diminished the

superiority of HF CDCs. In vivo, HF CDCs engrafted better (Figs. 6A and 6C) in post-MI mouse hearts and were more effective in recruiting endogenous stem cells (Figs. 7A to 7F), stimulating cardiomyocyte cell-cycle re-entry (Figs. 7G and 7H) and promoting angiogenesis (Figs. 7I and 7J). We also found that the SDF-1 levels of the 6 MI CDC lines correlated with their scar-limiting potency in patients (Fig. 8A). Engraftment 3 weeks after injection is low. However, it is notable that, during the 3-week course, the surviving cells may produce sufficient SDF-1, as well as other soluble factors, to trigger endogenous repair processes. Although the present data point to SDF-1 as a potential factor explaining disease-related potency differences, CDCs produce many factors other than SDF-1 as revealed by secretome (46) and ELISA analysis (9). These other factors likely play an important role in the overall therapeutic benefit of CDCs.

Why are failing hearts not able to spontaneously improve ventricular function with such robust HF-derived CDCs? It is known that the failing heart exhibits enhanced apoptosis (47) and oxidative stress (48). Thus, processes that favor cell death are up-regulated in HF, as is the regenerative potency of heart-derived cells. We speculate that the enhancement of cell death pathways offsets the enhanced regenerative capacity in the failing heart, such that the net result is neutral or perhaps negative, leading to net cardiomyocyte loss over time.

The mechanisms underlying the beneficial effects of stem cells are complex. CDC injection can stimulate new cardiomyocyte formation as well as vasculogenesis (9–12). Fate-mapping analysis reveals that, after CDC treatment, approximately half of newly formed cardiomyocytes arise from the proliferation of pre-existing myocytes, whereas the other half originate from endogenous stem cell recruitment (12). Here, we have found that HF CDCs secrete higher levels of SDF-1, which can promote new cardiomyocyte formation, angiogenesis, and stem cell recruitment, consistent with the observed superior cardioprotective/regenerative potency of the HF CDC-group. Nevertheless, future studies are needed to further dissect these mechanisms.

Study limitations

First, the sample size for each group is relatively small, making it difficult to match age, race, and sex; also, comorbidities vary, especially in the HF group (although the patients were uniformly NYHA functional class IV). The majority of CDC samples could be expanded for 6 to 10 passages. Very few CDC samples stopped growing at early passages (1 in 17). The rarity of failure to grow is true for all 3 CDC groups. Second, the NF donor hearts were exposed to immunosuppressive regimens and to an allogeneic environment, either of which could affect the performance of these CDCs. Nevertheless, we now have new data from perfectly normal hearts after accidental death. These hearts, obtained through the National Disease Research Interchange, yielded CDCs that produced a LVEF increase of 4.6% to 5.8% in the same mouse model of MI (data not shown). Because the increment in LVEF is similar to what we saw in the NF donor CDC group in the present paper, it appears that the transplanted donor hearts are indeed a relevant source of non-diseased tissue. Third, although the time in culture was similar for all groups (Fig. 1B), it is nevertheless possible that the in vitro expansion process may amplify differences between groups, and positively select “stronger” populations. Fourth, we did not explore directly whether SDF-1 itself can mediate the therapeutic benefits (i.e., by injecting recombinant SDF-1 alone and/or inhibiting SDF-1 in the HF group). However, previous studies have demonstrated the potential utility of SDF-1 as a therapeutic agent after myocardial infarction (49,50). Last, but not least, because of the intrinsic limitations of rodent studies (51), large-animal studies are required to validate these findings and to weigh the potential utility of HF CDCs in human trials.

Conclusions

CDCs from end-stage HF hearts were phenotypically similar to CDCs from healthy sources and were not compromised (rather, they were augmented) in their therapeutic benefit, possibly through SDF-1-mediated mechanisms. This paradoxical finding means that surgical discards from heart transplantation or device installation could be used as sources for therapeutic cells.

Supplementary Material

Refer to Web version on PubMed Central for supplementary material.

Acknowledgments

The authors thank Ms. Supurna Chowdhury, Ms. Doan Trang Duong, Ms. Janice Doldron, Ms. Tracey Early, and Mr. DeoMarie Sy for technical assistance.

This work was supported by grants from the National Institutes of Health and the California Institute for Regenerative Medicine to Dr. E. Marbán, an American Heart Association Beginning Grant-In-Aid to Dr. Cheng, and a fellowship from the International Society for Heart and Lung Transplantation to Dr. Malliaras. Dr. Malliaras receives consulting fees from Capricor, Inc. Dr. Smith and Ms. Blusztajn are employees of Capricor, Inc. Dr. L. Marbán is employed by Capricor, Inc.; is on the board of directors of Capricor, Inc.; and owns stock in Capricor, Inc. Dr. E. Marbán is a scientific advisor for and owns stock in Capricor, Inc.

Abbreviations and Acronyms

CDC	cardiosphere-derived cell
ELISA	enzyme-linked immunosorbent assay
HF	heart failure
HNA	human-specific nuclear antigen
LVEF	left ventricular ejection fraction
MI	myocardial infarction
NF	non-failing
NRCM	neonatal rat cardiomyocyte
NYHA	New York Heart Association
RT-PCR	reverse transcription–polymerase chain reaction
SDF-1	stromal cell-derived factor 1
TUNEL	terminal deoxynucleotidyl transferase dUTP nick end labeling

REFERENCES

1. Makkar RR, Smith RR, Cheng K, et al. Intracoronary cardiosphere-derived cells for heart regeneration after myocardial infarction (caduceus): a prospective, randomised phase 1 trial. *Lancet*. 2012; 379:895–904. [PubMed: 22336189]
2. White AJ, Smith RR, Matsushita S, et al. Intrinsic cardiac origin of human cardiosphere-derived cells. *Eur Heart J*. 2013; 34:68–75. [PubMed: 21659438]
3. Li TS, Cheng K, Malliaras K, et al. Direct comparison of different stem cell types and subpopulations reveals superior paracrine potency and myocardial repair efficacy with cardiosphere-derived cells. *J Am Coll Cardiol*. 2012; 59:942–53. [PubMed: 22381431]

4. Smith RR, Barile L, Cho HC, et al. Regenerative potential of cardiosphere-derived cells expanded from percutaneous endomyocardial biopsy specimens. *Circulation*. 2007; 115:896–908. [PubMed: 17283259]
5. Cheng K, Shen D, Smith J, et al. Transplantation of platelet gel spiked with cardiosphere-derived cells boosts structural and functional benefits relative to gel transplantation alone in rats with myocardial infarction. *Biomaterials*. 2012; 33:2872–9. [PubMed: 22243801]
6. Malliaras K, Li TS, Luthringer D, et al. Safety and efficacy of allogeneic cell therapy in infarcted rats transplanted with mismatched cardiosphere-derived cells. *Circulation*. 2012; 125:100–12. [PubMed: 22086878]
7. Terrovitis J, Lautamaki R, Bonios M, et al. Noninvasive quantification and optimization of acute cell retention by in vivo positron emission tomography after intramyocardial cardiac-derived stem cell delivery. *J Am Coll Cardiol*. 2009; 54:1619–26. [PubMed: 19833262]
8. Terrovitis JV, Smith RR, Marban E. Assessment and optimization of cell engraftment after transplantation into the heart. *Circ Res*. 2010; 106:479–94. [PubMed: 20167944]
9. Chimenti I, Smith RR, Li TS, et al. Relative roles of direct regeneration versus paracrine effects of human cardiosphere-derived cells transplanted into infarcted mice. *Circ Res*. 2010; 106:971–80. [PubMed: 20110532]
10. Cheng K, Li TS, Malliaras K, Davis DR, Zhang Y, Marban E. Magnetic targeting enhances engraftment and functional benefit of iron-labeled cardiosphere-derived cells in myocardial infarction. *Circ Res*. 2010; 106:1570–81. [PubMed: 20378859]
11. Cheng K, Malliaras K, Li TS, et al. Magnetic enhancement of cell retention, engraftment and functional benefit after intracoronary delivery of cardiac-derived stem cells in a rat model of ischemia/ reperfusion. *Cell Transplant*. 2012; 21:1121–35. [PubMed: 22405128]
12. Malliaras K, Zhang Y, Seinfeld J, et al. Cardiomyocyte proliferation and progenitor cell recruitment underlie therapeutic regeneration after myocardial infarction in the adult mouse heart. *EMBO Mol Med*. 2012; 5:191–209. [PubMed: 23255322]
13. Davis DR, Kizana E, Terrovitis J, et al. Isolation and expansion of functionally-competent cardiac progenitor cells directly from heart biopsies. *J Mol Cell Cardiol*. 2010; 49:312–1. [PubMed: 20211627]
14. Davis DR, Zhang Y, Smith RR, et al. Validation of the cardiosphere method to culture cardiac progenitor cells from myocardial tissue. *PLoS ONE*. 2009; 4:e7195. [PubMed: 19779618]
15. Johnston PV, Sasano T, Mills K, et al. Engraftment, differentiation, and functional benefits of autologous cardiosphere-derived cells in porcine ischemic cardiomyopathy. *Circulation*. 2009; 120:1075–83. [PubMed: 19738142]
16. Lee ST, White AJ, Matsushita S, et al. Intramyocardial injection of autologous cardiospheres or cardiosphere-derived cells preserves function and minimizes adverse ventricular remodeling in pigs with heart failure post-myocardial infarction. *J Am Coll Cardiol*. 2011; 57:455–65. [PubMed: 21251587]
17. Li TS, Cheng K, Lee ST, et al. Cardiospheres recapitulate a niche-like microenvironment rich in stemness and cell-matrix interactions, rationalizing their enhanced functional potency for myocardial repair. *Stem Cells*. 2010; 28:2088–98. [PubMed: 20882531]
18. Shen D, Cheng K, Marban E. Dose-dependent functional benefit of human cardiosphere transplantation in mice with acute myocardial infarction. *J Cell Mol Med*. 2012; 16:2112–6. [PubMed: 22225626]
19. Loffredo FS, Steinhilber ML, Gannon J, Lee RT. Bone marrow-derived cell therapy stimulates endogenous cardiomyocyte progenitors and promotes cardiac repair. *Cell Stem Cell*. 2011; 8:389–98. [PubMed: 21474103]
20. Tang XL, Rokosh G, Sanganalmath SK, et al. Intracoronary administration of cardiac progenitor cells alleviates left ventricular dysfunction in rats with a 30-day-old infarction. *Circulation*. 2010; 121:293–305. [PubMed: 20048209]
21. Kamihata H, Matsubara H, Nishiue T, et al. Implantation of bone marrow mononuclear cells into ischemic myocardium enhances collateral perfusion and regional function via side supply of angioblasts, angiogenic ligands, and cytokines. *Circulation*. 2001; 104:1046–52. [PubMed: 11524400]

22. Bergmann O, Bhardwaj RD, Bernard S, et al. Evidence for cardiomyocyte renewal in humans. *Science*. 2009; 324:98–102. [PubMed: 19342590]
23. Kajstura J, Gurusamy N, Ogórek B, et al. Myocyte turnover in the aging human heart. *Circ Res*. 2010; 107:1374–86. [PubMed: 21088285]
24. D'Amario D, Fiorini C, Campbell PM, et al. Functionally competent cardiac stem cells can be isolated from endomyocardial biopsies of patients with advanced cardiomyopathies. *Circ Res*. 2011; 108:857–61. [PubMed: 21330601]
25. Mishra R, Vijayan K, Colletti EJ, et al. Characterization and functionality of cardiac progenitor cells in congenital heart patients. *Circulation*. 2011; 123:364–73. [PubMed: 21242485]
26. Rupp S, Bauer J, von Gerlach S, et al. Pressure overload leads to an increase of cardiac resident stem cells. *Basic Res Cardiol*. 2012; 107:1–7.
27. Kubo H, Jaleel N, Kumarapeli A, et al. Increased cardiac myocyte progenitors in failing human hearts. *Circulation*. 2008; 118:649–57. [PubMed: 18645055]
28. Fortini C, Toffoletto B, Fucili A, et al. Circulating stem cell vary with nyha stage in heart failure patients. *J Cell Mol Med*. 2011; 15:1726–36. [PubMed: 21029373]
29. Theiss HD, David R, Engelmann MG, et al. Circulation of cd34+ progenitor cell populations in patients with idiopathic dilated and ischaemic cardiomyopathy (DCM and ICM). *Eur Heart J*. 2007; 28:1258–64. [PubMed: 17395679]
30. Frangogiannis NG. The stromal cell-derived factor-1/CXCR4 axis in cardiac injury and repair. *J Am Coll Cardiol*. 2011; 58:2424–6. [PubMed: 22115650]
31. Ghadge SK, Mühlstedt S, Özcelik C, Bader M. Sdf-1a as a therapeutic stem cell homing factor in myocardial infarction. *Pharmacol Ther*. 2011; 129:97–108. [PubMed: 20965212]
32. Hu X, Dai S, Wu W-J, et al. Stromal cell-derived factor-1a confers protection against myocardial ischemia/reperfusion injury. *Circulation*. 2007; 116:654–63. [PubMed: 17646584]
33. Saxena A, Fish JE, White MD, et al. Stromal cell-derived factor-1a is cardioprotective after myocardial infarction. *Circulation*. 2008; 117:2224–31. [PubMed: 18427137]
34. Segers VFM, Tokunou T, Higgins LJ, MacGillivray C, Gannon J, Lee RT. Local delivery of protease-resistant stromal cell derived factor-1 for stem cell recruitment after myocardial infarction. *Circulation*. 2007; 116:1683–92. [PubMed: 17875967]
35. Askari AT, Unzek S, Popovic ZB, et al. Effect of stromal-cell-derived factor 1 on stem-cell homing and tissue regeneration in ischaemic cardiomyopathy. *Lancet*. 2003; 362:697–703. [PubMed: 12957092]
36. Deshane J, Chen S, Caballero S, et al. Stromal cell-derived factor 1 promotes angiogenesis via a heme oxygenase 1-dependent mechanism. *J Exp Med*. 2007; 204:605–18. [PubMed: 17339405]
37. Kanda S, Mochizuki Y, Kanetake H. Stromal cell-derived factor-1a induces tube-like structure formation of endothelial cells through phosphoinositide 3-kinase. *J Biol Chem*. 2003; 278:257–62. [PubMed: 12414810]
38. Petit I, Jin D, Rafii S. The SDF-1 CXCR4 signaling pathway: a molecular hub modulating neo-angiogenesis. *Trends Immunol*. 2007; 28:299–307. [PubMed: 17560169]
39. Guo Y, Hangoc G, Bian H, Pelus LM, Broxmeyer HE. SDF-1/ CXCL12 enhances survival and chemotaxis of murine embryonic stem cells and production of primitive and definitive hematopoietic progenitor cells. *Stem Cells*. 2005; 23:1324–32. [PubMed: 16210409]
40. Huang C, Gu H, Zhang W, Manukyan MC, Shou W, Wang M. SDF-1/CXCR4 mediates acute protection of cardiac function through myocardial stat3 signaling following global ischemia/reperfusion injury. *Am J Physiol Heart Circ Physiol*. 2011; 301:H1496–505. [PubMed: 21821779]
41. Jaleel MA, Tsai AC, Sarkar S, Freedman PV, Rubin LP. Stromal cell-derived factor-1 (sdf-1) signalling regulates human placental tropho-blast cell survival. *Mol Hum Reprod*. 2004; 10:901–9. [PubMed: 15475370]
42. Kortesisidis A, Zannettino A, Isenmann S, Shi S, Lapidot T, Gronthos S. Stromal-derived factor-1 promotes the growth, survival, and development of human bone marrow stromal stem cells. *Blood*. 2005; 105:3793–801. [PubMed: 15677562]
43. Lataillade J-J, Clay D, Dupuy C, et al. Chemokine SDF-1 enhances circulating CD34+ cell proliferation in synergy with cytokines: possible role in progenitor survival. *Blood*. 2000; 95:756–68. [PubMed: 10648383]

44. Abbott JD, Huang Y, Liu D, Hickey R, Krause DS, Giordano FJ. Stromal cell-derived factor-1 α plays a critical role in stem cell recruitment to the heart after myocardial infarction but is not sufficient to induce homing in the absence of injury. *Circulation*. 2004; 110:3300–5. [PubMed: 15533866]
45. Zakharova L, Mastroeni D, Mutlu N, et al. Transplantation of cardiac progenitor cell sheet onto infarcted heart promotes cardiogenesis and improves function. *Cardiovas Res*. 2010; 87:40–9.
46. Stastna M, Chimenti I, Marbán E, Van Eyk JE. Identification and functionality of proteomes secreted by rat cardiac stem cells and neonatal cardiomyocytes. *Proteomics*. 2010; 10:245–53. [PubMed: 20014349]
47. Jiang L, Huang Y, Hunyor S, dos Remedios CG. Cardiomyocyte apoptosis is associated with increased wall stress in chronic failing left ventricle. *Eur Heart J*. 2003; 24:742–51. [PubMed: 12713768]
48. Grieve DJ, Shah AM. Oxidative stress in heart failure. *Eur Heart J*. 2003; 24:2161–3. [PubMed: 14659766]
49. Penn MS, Pastore J, Miller T, Aras R. SDF-1 in myocardial repair. *Gene Ther*. 2012; 19:583–7. [PubMed: 22673496]
50. Penn MS. Importance of the SDF-1:CXCR4 axis in myocardial repair. *Circ Res*. 2009; 104:1133–5. [PubMed: 19461103]
51. Zaragoza C, Gomez-Guerrero C, Martin-Ventura JL, et al. Animal models of cardiovascular diseases. *J Biomed Biotech*. 2011; 2011:497841.

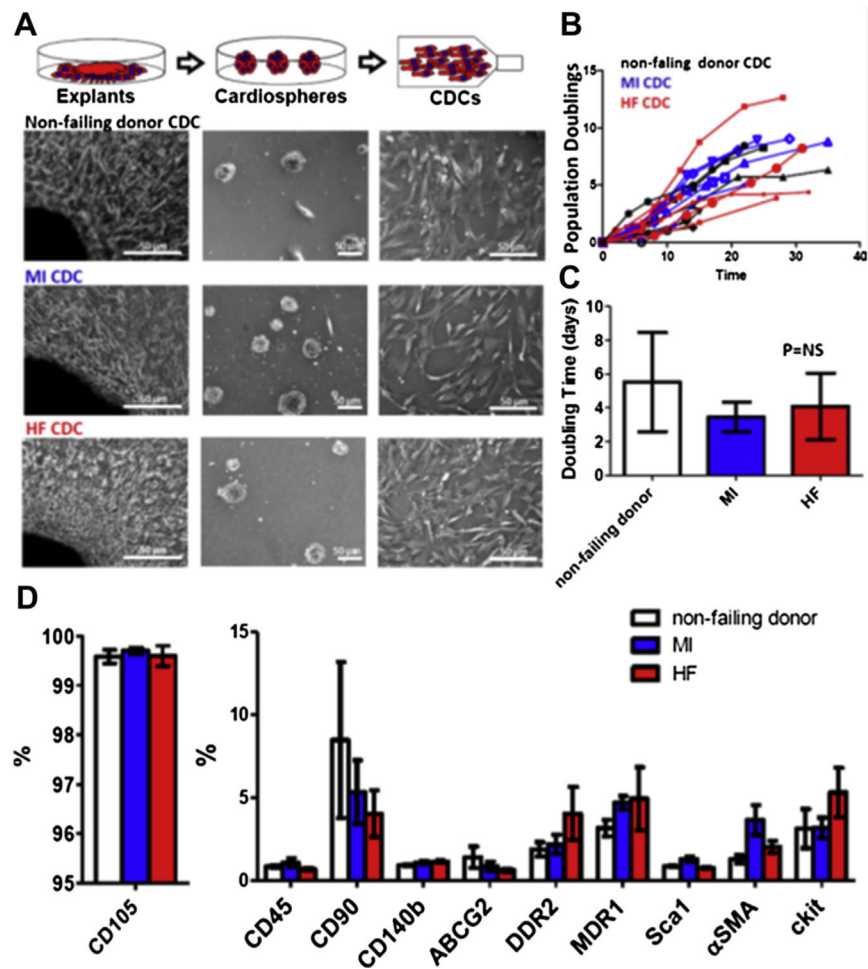


Figure 1. Characteristics of CDCs Derived From Patients

(A) Schematic showing the process of deriving cardiosphere-derived cells (CDCs) from myocardial tissue. (B) Population doubling over time in non-failing (NF) donor, myocardial infarction (MI), and heart failure (HF) CDCs. (C) Average doubling time of NF donor, MI, and HF CDCs (n = 6 patient-derived CDC lines). (D) Summary of antigenic phenotype of CDCs. Data are presented as means \pm SD.

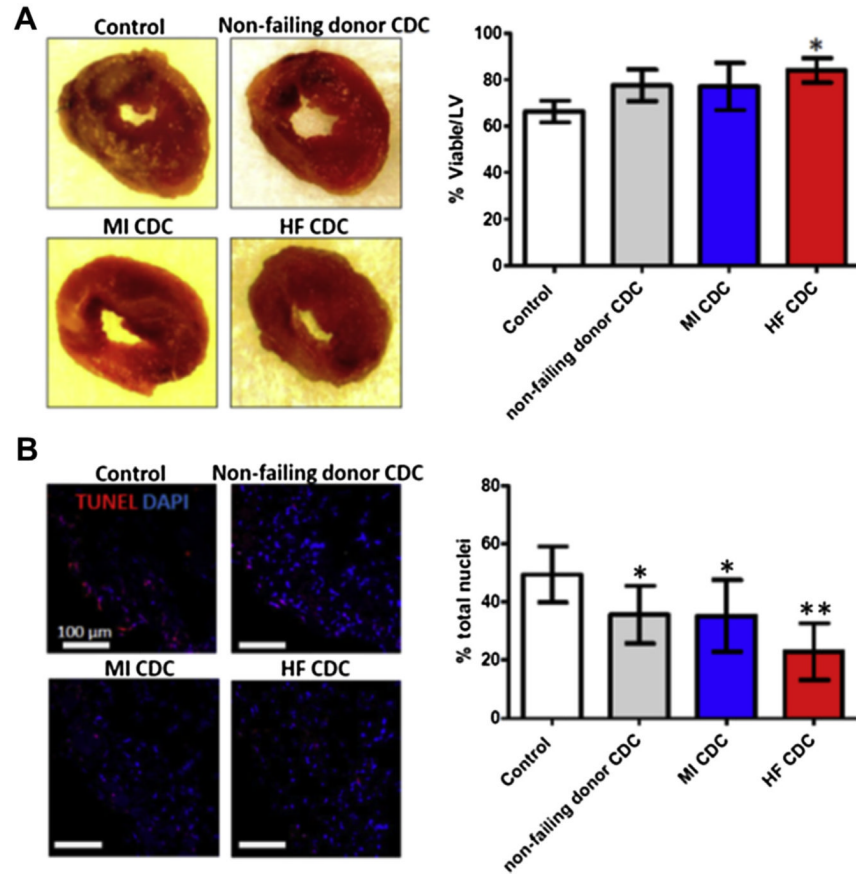


Figure 2. Acute Cardioprotective Effects of Injected CDCs

(A) Representative macroscopic images of hearts from each experimental group after TTC staining (**left**). Pale areas are irreversibly injured. **Right panel** shows pooled data for the percentage viability. (B) Representative confocal images showing terminal deoxynucleotidyl transferase dUTP nick end labeling (TUNEL) staining for apoptotic nuclei in the infarct area 24 h after myocardial infarction (**left**), and pooled data (**right**). * $p < 0.05$ compared with Control; ** $p < 0.05$ compared with all other groups. Data are presented as means \pm SD. Abbreviations as in Figure 1.

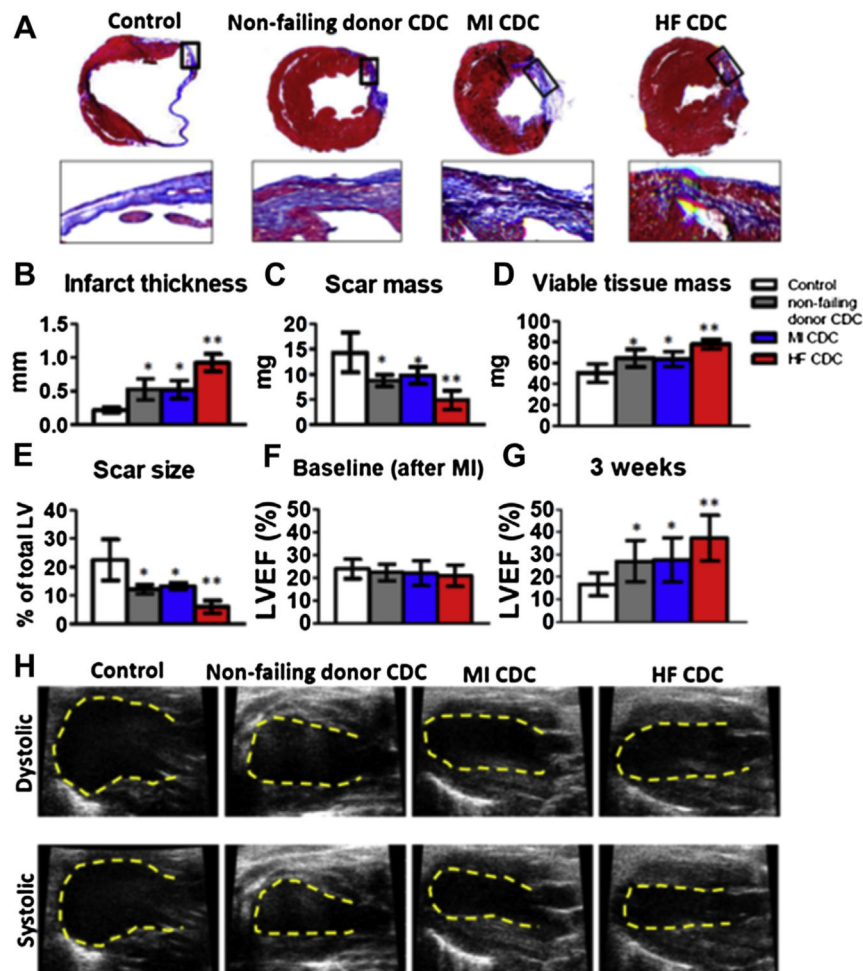


Figure 3. Therapeutic Benefit of NF Donor, MI, and HF CDCs in Mice With MI
 (A) Representative Masson's trichrome–stained myocardial sections 3 weeks after treatment with Control (vehicle only), NF donor, MI, and HF CDCs. Scar tissue and viable myocardium are identified by the **blue** and **red** colors, respectively. Snapshots of the infarct border zone (**black box area**) are presented beneath each group. (B–E) Quantitative analysis of infarct thickness, scar mass, viable tissue mass, and scar size from the Masson's trichrome–stained images ($n = 6$ animals per group). Left ventricular ejection fraction (LVEF) was measured by echocardiography at baseline (4 h post-MI) (F) and 3 weeks afterwards (G) (Control: $n = 11$ animals; NF donor, MI, or HF CDC: $n = 19$ to 24 animals from $n = 6$ patient-derived CDC lines). Baseline LVEFs were indistinguishable in the 4 groups. (H) Representative echocardiography images. * $p < 0.05$ compared with Control; ** $p < 0.05$ compared with all other groups. Data are presented as means \pm SD. Abbreviations as in Figure 1.

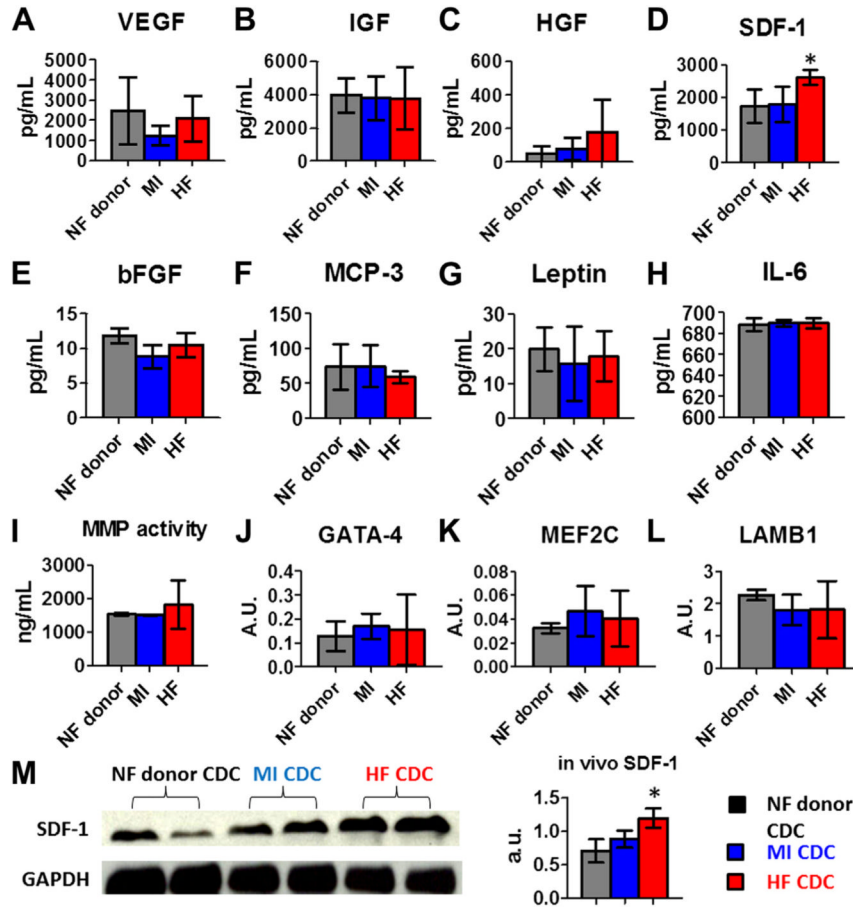


Figure 4. Paracrine Factors and Gene Expression in CDCs
 (A–H) Secretion of various cytokines and growth factors from NF donor, MI, and HF CDCs. Concentrations were measured by enzyme-linked immunosorbent assay (ELISA). (I) Proteinolytic activity (MMP2/MMP9) in CDC-conditioned media. (J–L) *GATA4*, *MEF2C*, and laminin beta 1 (*LAMB1*) transcript levels in CDCs measured by reverse transcription–polymerase chain reaction (RT-PCR) (n = 6 for each group). (M) Western blot analysis of myocardial SDF-1 (representative blot, left, and pooled data, right; n = 4 per group). *p < 0.05 compared with the other 2 groups. Data are presented as means ± SD. Abbreviations as in Figure 1.

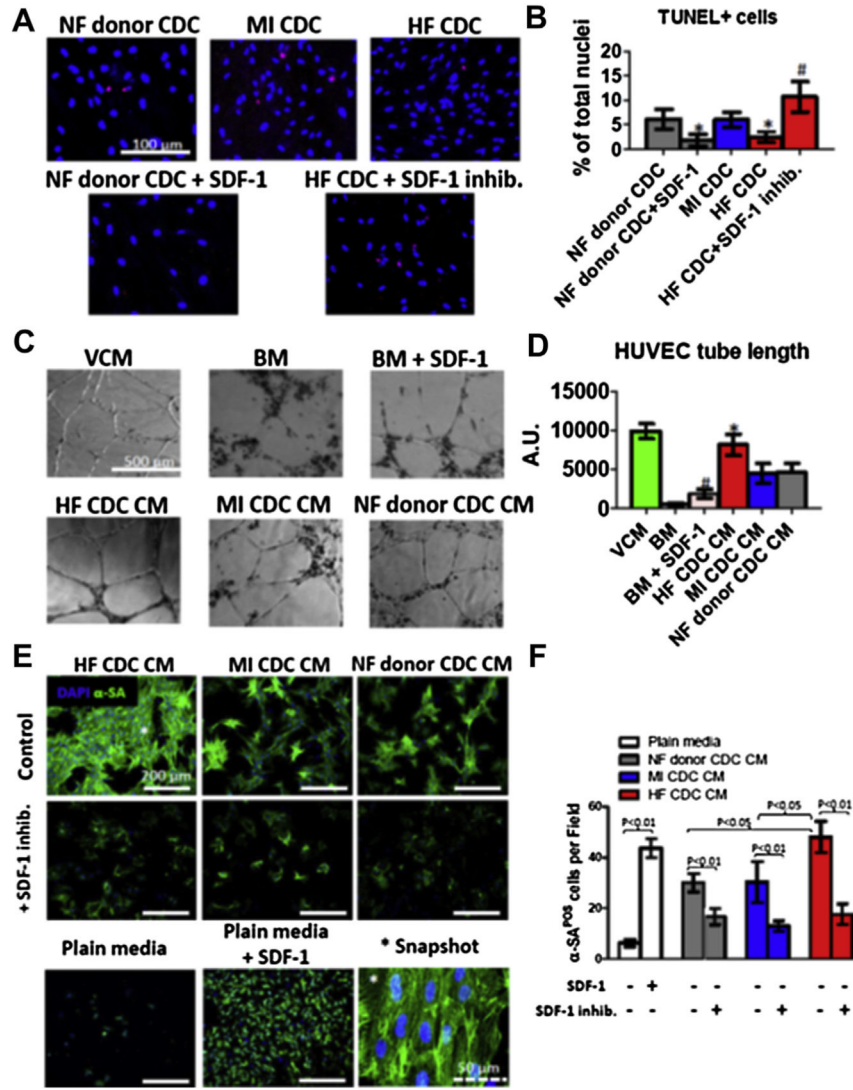


Figure 5. Resistance to Oxidative Stress, Endothelial Cell Angiogenesis, and Cardiomyocyte Survival and Contractile Assays
 (A) Representative confocal fluorescent micrographs showing TUNEL⁺ nuclei (red) in CDC cultures exposed to 100 μmol/l H₂O₂. (B) Quantification of the percentages of TUNEL⁺ cells in NF donor, MI, and HF CDCs (n = 6). *p < 0.05 compared with the NF donor CDC group; #p < 0.05 compared with the HF CDC group. (C) Representative white light images showing tube formation by human umbilical vein endothelial cells (HUVECs) on Matrigel in various types of media. BM = vascular cell basal medium; VCM = vascular cell growth medium. (D) Cumulative tube length measured by Image-Pro Plus (MediaCybernetics, Rockville, Maryland) in each well (n = 3). *p < 0.05 when compared with NF donor CDC CM group; #p < 0.05 when compared with the BM group. A.U. = arbitrary units. (E) Representative confocal images showing neonatal rat cardiomyocytes stained with α-sarcomeric actin in different culture conditions. (F) Numbers of cardiomyocytes per field under each condition (n = 3). Data are presented as means ± SD. CM = conditioned medium; other abbreviations as in Figures 1 and 3.

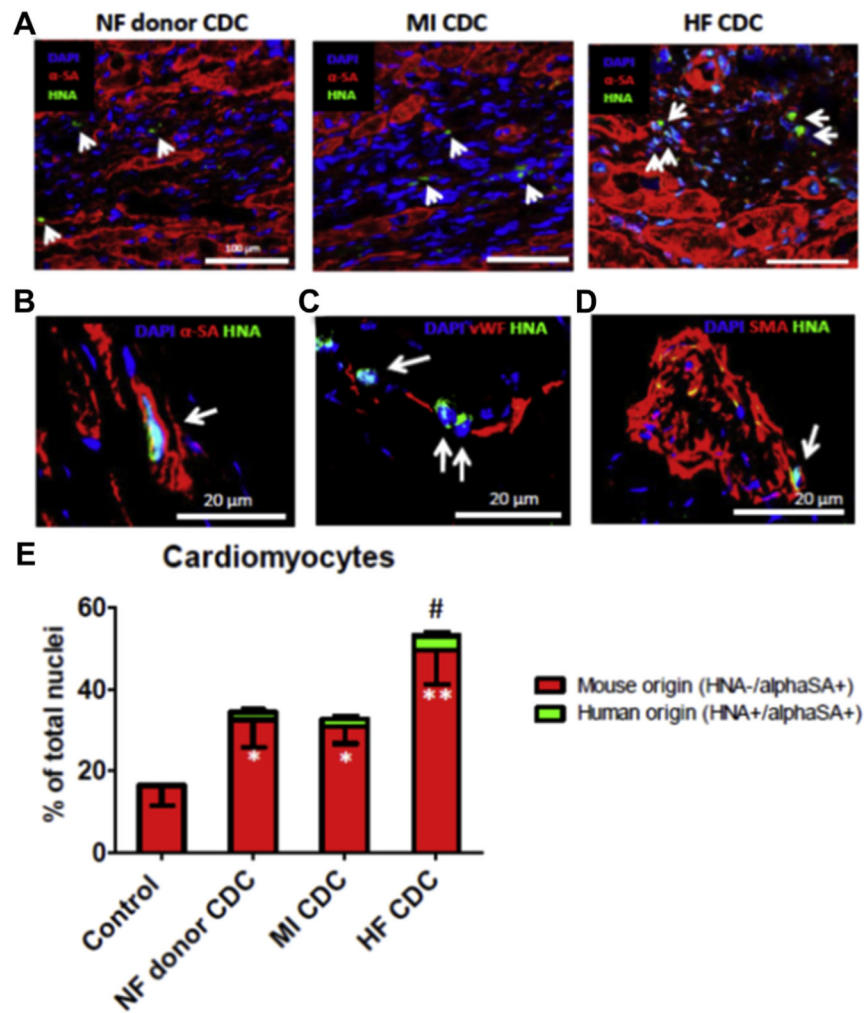


Figure 6. Engraftment and Differentiation of Transplanted Cells and New Cardiomyocyte Formation

(A) Representative confocal images showing the engraftment of transplanted CDCs (positive for human nuclei antigen [HNA]; **green**, indicated by **white arrows**) in the infarct border zone. Cardiomyocytes were stained with alpha-sarcomeric actin (α -SA; **red**). (B–D), Co-expression of HNA (**green**) with α -SA, von Willebrand factor (vWF), alpha-smooth muscle actin (SMA) in HF CDCs (**white arrows**) in mouse hearts. (E) Quantification of endogenous (α -SA⁺/HNA⁻) and exogenous (α -SA⁺/HNA⁺) cardiomyocytes in the peri-infarct area. * $p < 0.05$ compared with Control; ** $p < 0.05$ compared with all other groups; # $p < 0.05$ compared with the NF donor CDC or MI CDC group. Data are presented as means \pm SD. Abbreviations as in Figure 1.

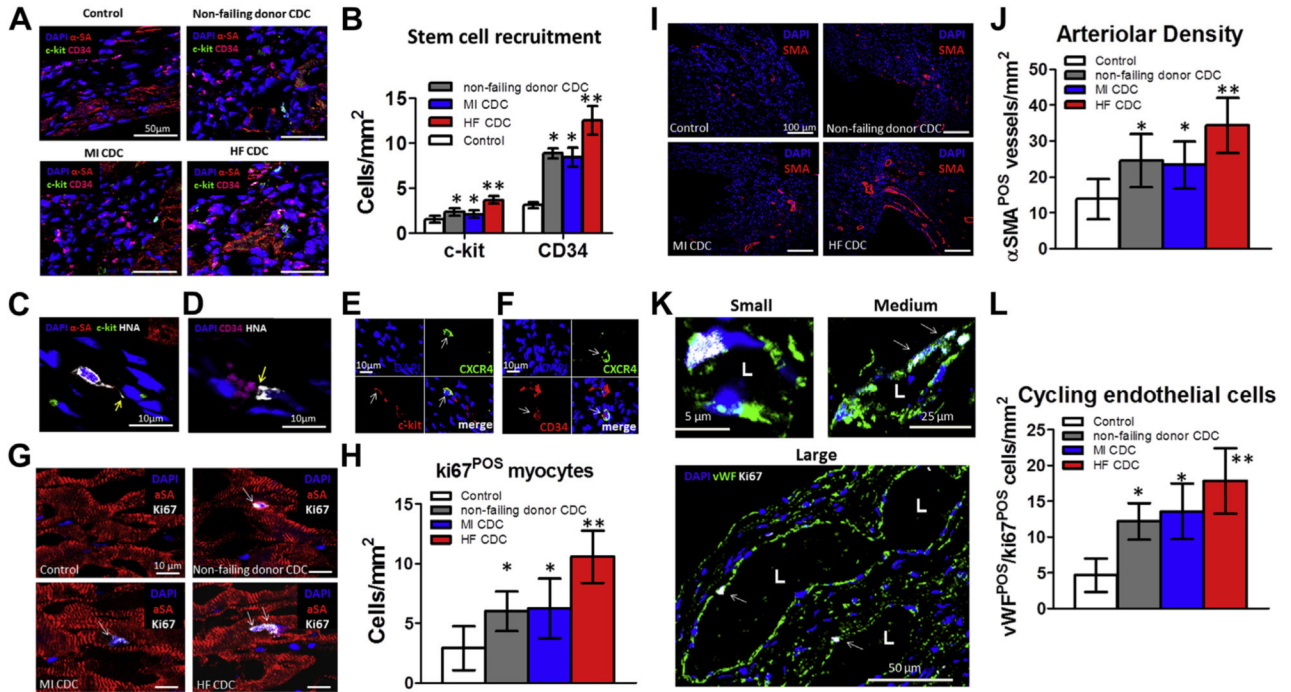


Figure 7. Recruitment of Stem Cells, Cardiomyocyte Cell-Cycle Re-Entry, and Angiogenesis
(A) Representative confocal images showing c-kit⁺ (green) and CD34⁺ (magenta) stem cells in the infarct border zone. Cardiomyocytes were stained with alpha-sarcomeric actin (α-SA; red). **(B)** Quantitation of c-kit⁺ and CD34⁺ cells (n = 3 hearts per group). *p < 0.05 compared with Control; **p < 0.05 compared with all other groups. Large magnification revealed interactions (yellow arrow) between transplanted HF CDCs with c-kit⁺ (C) or CD34⁺ cells (D). **(E)** Co-expression of CXCR4 (green) in c-kit⁺ cells (red). **(F)** Co-expression of CXCR4 (green) in CD34⁺ cells (red). **(G)** Cardiomyocytes (stained with α-SA; red) containing Ki67⁺ nuclei (white) in the infarct border zone. **(H)** Quantitation of Ki67⁺ cardiomyocytes in each group (n = 3 hearts per group). **(I)** Arteriolar structures stained with SMA (red) in the infarct border zone. **(J)** Quantitation of arteriolar density in each group (n = 3 hearts per group). **(K)** cycling endothelial cells stained with ki67 (white) and vWF (green). **(L)** Quantitation of cycling endothelial cells in each group (n = 3 hearts per group). *p < 0.05 compared with Control; **p < 0.05 compared with all other groups. Data are presented as means ± SD. Abbreviations as in Figures 1 and 6.

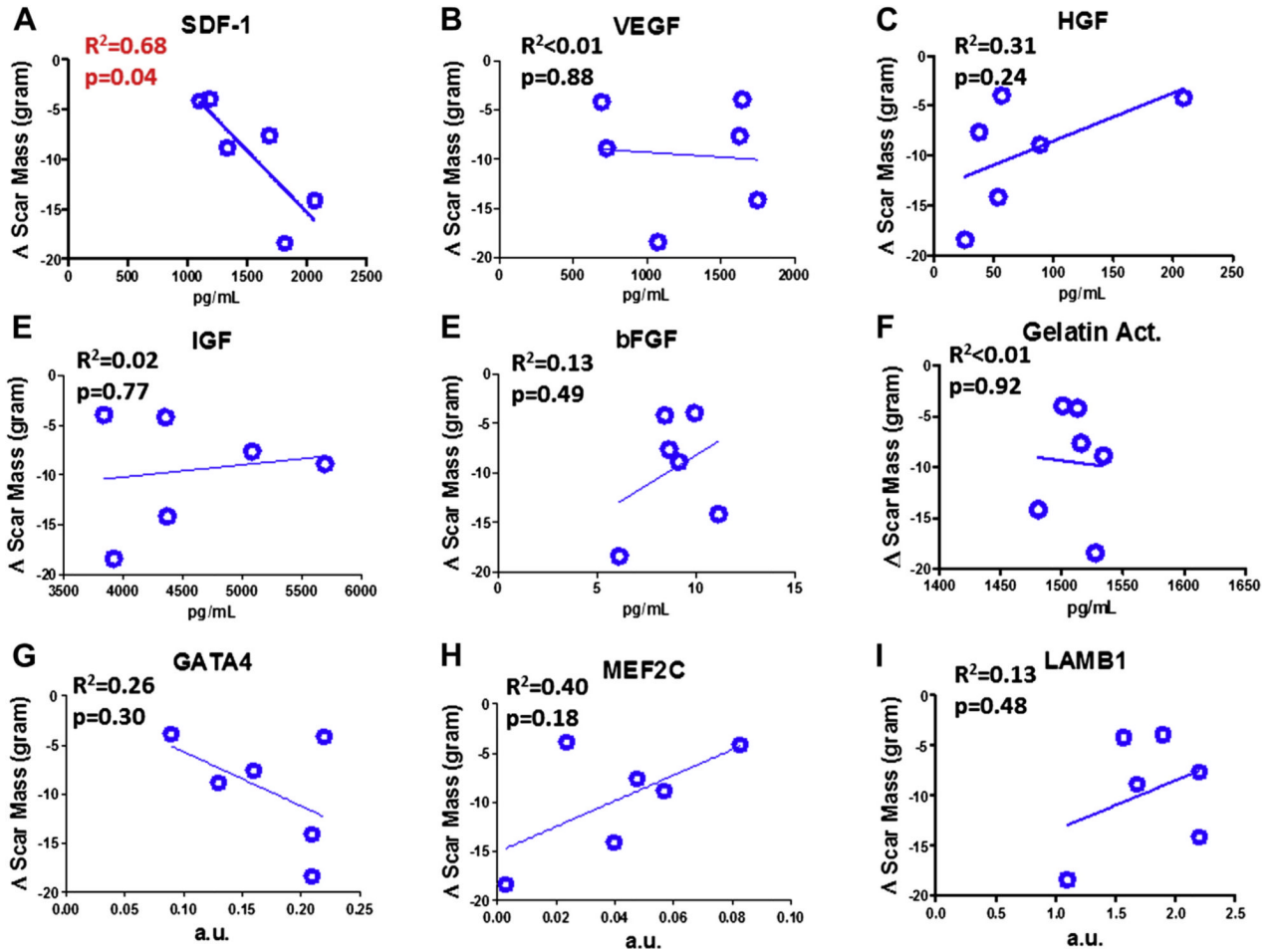


Figure 8. Correlation of CDC Properties With Scar Mass Changes in CADUCEUS Patients
 Linear regression analysis was performed to reveal the relationship between various paracrine factors/gene expression levels and the changes of the patients’ cardiac scar tissue mass over the 6-month follow-up. Only SDF-1 levels reveal a significant correlation with decreasing scar mass. Data are presented as means ± SD. a.u. = arbitrary units; CADUCEUS = CARDiosphere-Derived aUtologous stem CELls to reverse ventricUlar dysfunction.

Table 1

Patient Characteristics

HF CDC Patients									
ID	Sex	Age (Yrs)	Race	Etiology		HTN	DM	CHOL	NYHA
#1	M	61	Hispanic	Restrictive cardiomyopathy secondary to amyloidosis		Yes	No	No	IV
#2	F	29	Caucasian	Arrhythmogenic right ventricular dysplasia		No	No	No	IV
#3	M	67	Caucasian	Ischemic dilated cardiomyopathy		Yes	No	Yes	IV
#4	M	69	Asian/Pacific Islander	Idiopathic dilated cardiomyopathy		Yes	No	Yes	IV
#5	F	52	Caucasian	Ischemic dilated cardiomyopathy		Yes	Yes	No	IV
#6	M	48	Hispanic	Ischemic dilated cardiomyopathy and possible Chagas' disease		Yes	Yes	Yes	IV

MI CDC Patients									
ID	Sex	Age (Yrs)	Race	Days to Biopsy	Etiology	HTN	DM	CHOL	NYHA
#1	M	58	Caucasian	20	Acute myocardial infarction	Yes	No	Yes	II
#2	M	46	Caucasian	9	Acute myocardial infarction	Yes	No	Yes	I
#3	M	60	Caucasian	35	Acute myocardial infarction	No	No	Yes	II
#4	M	70	Caucasian	25	Acute myocardial infarction	Yes	No	Yes	II
#5	M	54	Caucasian	16	Acute myocardial infarction	No	Yes	Yes	I
#6	M	55	Caucasian	27	Acute myocardial infarction	Yes	No	Yes	I

Normal CDC (NF Donor Hearts)				
ID	Sex	Age (Yrs)	Race	Cause of Death
#1	M	36	Caucasian	Stroke/CVA
#2	M	43	Hispanic	Head trauma/motor vehicle accident
#3	M	18	Hispanic	Head trauma/motor vehicle accident
#4	M	53	Hispanic	Vehicular trauma
#5	M	36	Hispanic	Stroke
#6	M	41	Caucasian	Head trauma/motor vehicle accident

CDC = cardiosphere-derived cell; CHOL = hypercholesterolemia; CVA = cerebral vascular accident; DM = diabetes mellitus; F = female; HF = heart failure; HTN = hypertension; M = male; NF = non-failing; NYHA = New York Heart Association functional class.